Arabian Journal of Geosciences (2020) 13: 493
https://doi.org/10.1007/s12517-020-05555-9

ORIGINAL PAPER

Monitoring and investigating the possibility of forecasting drought in the western part of Iran

Vahid Safarian Zengir[1] · Behrouz Sobhani[1] · Sayyad Asghari[1]

Received: 24 October 2019 / Accepted: 4 June 2020 / Published online: 17 June 2020

Abstract

Drought is not specific to a particular region and is affecting different parts of the world, one of these areas being the western half of Iran, which has been suffering from this phenomenon in the recent years. The western half of Iran has been affected by natural hazards in the recent decades. One of these natural hazards is reduced rainfall, which manifests itself in the form of drought. The effects of drought in the different parts of the human society have been strongly felt in the recent years. Therefore, it is important to address this issue. The purpose of this study is to monitor and analyze drought in the western part of Iran. To do this, the MODIS satellite data, the NDVI (normalized difference vegetation index), and the TRMM (Tropical Rainfall Measurement Mission Project) satellite were used from 2000 to 2018, and for better analysis, they were compared with the fuzzy index of T.I.B.I (combined index based on four indices: SET, SPI, SEB, and MCZI) neural network. To calculate the T.I.B.I index, the ground climate parameters of precipitation, temperature, sunshine, minimum relative humidity, and wind speed were used; to extract satellite data and images, Google Earth Engine was used. The results of the study indicate that drought has started to weaken in the western part of Iran since 2010, and in 2016 and in the recent years, it has reached its peak. The northern and central regions of the study area were more prone to drought than elsewhere. Approximately 69.80% of the area is subject to severe drought. In order to deal with the catastrophe caused by drought that has many dangerous effects, it requires careful planning in the future.

Keywords Soil moisture · Evaporation and transpiration · Satellite meteorology · Drought sensitivity index

Introduction

Problems with water scarcity were caused by natural and human factors. They can have irreversible effects on human life, other living things, and the environment at the regional and trans-regional levels. Creating and exacerbating water scarcity crises can have adverse effects on the economy, society, and agriculture (Sobhani and Safarianzengir 2019a; Sobhani et al. 2019b). The frequency, severity, and extent of drought are very important aspects. Given the issues and problems caused by drought, monitoring and prediction for precision prevention and planning to control the risk of future drought in the region and its probability of occurrence by using precise model and method are essential. The southwestern and western parts of Iran are some of the areas that have not been protected from this risky phenomenon in the recent years. Studying this risky phenomenon in these areas is of great importance (Sobhani et al. 2019a; Sobhani et al. 2018; Feng et al. 2019). Among these climate-related extremes, droughts are a major threat, which have chronic, unpredictable, and random characteristics (Li et al. 2015; Zhang and Zhang 2016; Yuan et al. 2017). Drought is the most important disaster that reduces grain production in China, which has been affected by global warming in the recent years (Harrison et al. 2014; Piao et al. 2010; Campana et al. 2018; Yao et al. 2018; Feng et al. 2019). Hazard is defined as the potential occurrence of a natural or human-induced physical event or trend or physical impact that may cause loss of life, injury, or other health impacts, as well

Responsible Editor: Zhihua Zhang

✉ Behrouz Sobhani
behroz.sobhani@yahoo.com

Vahid Safarian Zengir
V.safarian@uma.ac.ir

Sayyad Asghari
Sayad.Asghariss@yahoo.com

[1] Faculty of Literature and Humanities, University of Mohaghegh Ardabili, Ardabil, Iran

as damage and loss to property, infrastructure, livelihoods, service provision, ecosystems, and environmental resources (IPCC 2014). Dozens of indices have been developed to quantify the duration, intensity, severity, and spatial extent of the drought hazard. These indices can be divided into two categories including univariate and multivariate (and bivariate) indices (Liu et al. 2019). The coincidence of the peaks of the scaling exponent with drought events suggests the increase of the persistence of the hot pixel time series during the driest periods (Stosic et al. 2015; Safarianzengir et al. 2019; Safarianzengir and Sobhani 2020). More intense and prolonged droughts will result in ecological degradation (Han et al. 2018). Variations in water fluxes are in large part due to the changes in evapotranspiration (ET), which is water loss via soil surface evaporation (E) and plant transpiration (T) (Fisher et al. 2008; Zhang et al. 2016; Han et al. 2018). More intense and persistent droughts are projected to cause major shifts in key processes in the water cycle, which in turn will affect the carbon and nitrogen cycles in terrestrial ecosystems (Corners et al. 2016; Sobhani and Safarianzengir 2020; Sobhani et al. 2020). When surface water availability is reduced during the dry seasons, groundwater demand increases (Thomas et al. 2019; Sobhani et al. 2019c). A recent study (Borromeo et al. 2018) estimated that a rainfall decrease could lead to a 10% decline in the agricultural gross domestic product (GDP) and a 5% decline in the overall regional GDP. This study estimated greater negative impacts among poorer households. When drought occurs, these vulnerable populations are highly reliant on groundwater supply to meet their basic needs, typically by utilizing boreholes pumping deep groundwater (Worqlul et al. 2017, Okotto et al. 2015; Thomas et al. 2019; Sobhani and Safarianzengir 2019b; Sobhani et al. 2020b; Tadesse et al. 2005; Jiao et al. 2019a, 2019b). There is an increasing need for comprehensive and reliable drought monitoring to aid planning and mitigation of drought impacts since the frequency and consequences of droughts are expected to intensify under climate change (Halwatura et al. 2017; Keyantash and Dracup 2004; Wilhelmi and Wilhite 2002; Zhou et al. 2012; Jiao et al. 2019a, b). More recently, global and near-real-time observations of remote sensing technology open the door for comprehensively characterizing drought conditions regionally and globally, especially in regions with limited sampling gauges (Jiao et al. 2019a, 2019b; Lu et al. 2016a, 2016b; Wang et al. 2012; Wu et al. 2013; Zhang et al. 2017; Jiao et al. 2019a, 2019b). Model data suggested that drought-related declines in LUE (living unit equivalent) for fluorescence and photosynthesis in areas of mixed forest produce losses in solar-induced fluorescence (SIF) and gross primary production (GPP) (Yoshida et al. 2015a, b). Satellite measurement of SIF from chlorophyll has emerged over the last few years as a different method to monitor vegetation globally from space (e.g., Frankenberg et al. 2011; Guanter et al. 2007, 2012; Joiner et al. 2011, 2012; Yoshida et al. 2015a, 2015b). Droughts and heatwaves have been and will continue to bring large risks to terrestrial ecosystems. However, the understanding of how plants respond to drought and heatwave over broad spatial scales is still limited (Wang et al. 2019). Drought and heatwave, which are associated with below-normal precipitation or above-normal air temperatures sustained for months to years, have substantial impacts on agriculture, water resources, and human society. The occurrence and duration of droughts and heatwaves have substantially increased as a consequence of climate change (Dai 2013; Trenberth et al. 2014; Wang et al. 2017a, 2017b; Wang et al. 2019). In Amazon, the drought induced by a strong El Niño event during 2015 and 2016 strongly decreased the GPP and resulted in reductions in the net carbon uptake of terrestrial ecosystems (Qian et al. 2019; Yang et al. 2018; Wang et al. 2019). Satellite-based SIF data have also been shown to be more sensitive to environmental stress than greenness-based VIs (Guan et al. 2016; Lee et al. 2013; Sun et al. 2015; Yoshida et al. 2015a, b). Global food security is negatively affected by drought. Climate projections show that drought frequency and intensity may increase in the different parts of the globe (Zambrano et al. 2018). Although increased levels of carbon dioxide in the atmosphere may increase the water use efficiency of crops (Donohue et al. 2013; Lu et al. 2016a, b), the combined effects of global mean temperature (Zhao et al. 2017) and drought occurrence (Dai 2012) are expected to cause an overall reduction in global crop yields (Ray et al. 2015; Zhao et al. 2017) and may have a negative impact on cropping frequency and sown area (Cohn et al. 2016; Zambrano et al. 2018). The most commonly used vegetation index for this purpose is the NDVI (normalized difference vegetation index; Rouse Jr. et al. 1974) from which multiple anomaly measures have been derived (Jiao et al. 2016; Kogan 1990; Peters et al. 2002a, 2002b; Sandholt et al. 2002) and applied for monitoring agricultural drought (Cunha et al. 2015; McVicar and Jupp 1998; Rojas et al. 2011; Zambrano et al. 2016; Zhang and Jia 2013; Zambrano et al. 2018). Other satellite-derived products that have relevance for drought monitoring include estimates of soil moisture and evapotranspiration (Hao and AghaKouchak 2013; Mu et al. 2013; Sheffield et al. 2004; Tsakiris et al. 2007). The untimely onset and uneven distribution of southwest monsoon rainfall lead to agricultural drought (Swapnil et al. 2015). The normalized difference vegetation index (NDVI) (Tucker 1979) is often used for monitoring drought. Reduction in seasonal NDVI was found to have a strong link with higher drought severity (Bajgirana et al. 2008; Thenkabail et al. 2004). There are also other indices used such as vegetation health index (VHI) (Kogan 2001), enhanced vegetation index (EVI) (Kogan 1997; Swapnil et al. 2015), vegetation temperature condition index (VTCI) (Wang et al. 2004), standardized vegetation index (SVI) (Peters et al. 2002a, b), and vegetation condition albedo

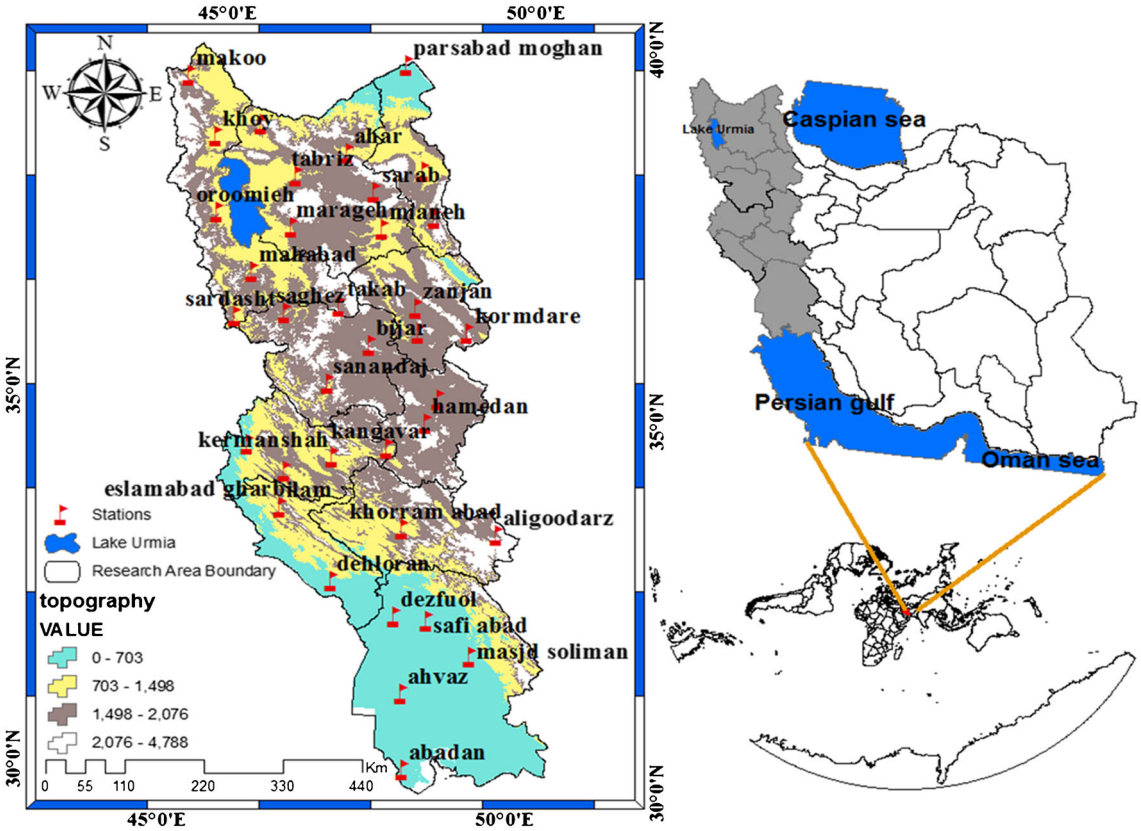

Fig. 1 Map of the study area showing the western part of Iran

drought index (VCADI) (Ghulam et al. 2007). Since the effects of drought show up over time and slowly, its effects may be minimized. However, this atmospheric phenomenon has a long and severe effect on plants, animals, and people. The effects of drought are more significant in three areas, which have many detrimental effects: society, economy, and environment. Therefore, it is important to address this issue. According to these studies, the purpose of the present study is to monitor and forecast drought in the western part of Iran.

Materials and methods

Study area

In the present study, 36 synoptic stations in the western part of Iran were studied It has 30 years of terrestrial climate data and 19 years of data satellite. In 10 provinces (East Azerbaijan, West Azerbaijan, Ardabil, Zanjan, Kurdistan, Hamedan, Kermanshah, Ilam, Lorestan, and Khuzestan), between the coordinates 30° 06′ 52″ to 39° 48′ 55″ North and 44° 04′ 43″ to 49° 50′ 76″ East. The location of the study area and the stations are presented in Fig. 1. To calculate the T.I.B.I)combined index based on four indices: SET, SPI, SEB, and MCZI) ,climatic parameters (precipitation, temperature, sunshine, minimum relative humidity, and wind speed) were used.

The standardized precipitation evapotranspiration new fuzzy index (T.I.B.I)

The new fuzzy climatic index T.I.B.I)combined index based on four indices: SET, SPI, SEB, and MCZI) is presented to correct some of the disadvantages of the SPEI (combining indicators: SPI and SEI) index. The fuzzy index (T.I.B.I)

Table 1 Classification of drought and wet year severity based on fuzzy modeling of T.I.B.I index

Drought classes	The index value of T.I.B.I
Very severe drought	0.96–1
Severe drought	0.87–0.96
Moderate drought	0.74–0.87
Mild drought	0.59–0.74
Normal drought	0.44–0.59
Mild wet season	0.29–0.44
Moderate wet season	0.15–0.29
Severe wet season	0.06–0.15
Very severe wet season	0–0.06

Fig. 2 The general architecture of the fuzzy model of drought monitoring

was obtained by combining the four indices of SET (standardized evapotranspiration torrent white index), SPI (standardized precipitation index), SEB (standardized evapotranspiration Blanney Creedal FAO Index), and MCZI (Modified CZI Index) in the fuzzy inference system. To calculate the T.I.B.I index, the first four indices were calculated. After calculating the four indices according to the method described in T.I.B.I (Table 1), they were evaluated; the architecture of the fuzzy model of drought monitoring is shown in Fig. 2.

ANFIS (adaptive neuro-fuzzy inference system) neural network model

In this step, the possibility of modeling and prediction of dust was studied in the study area using the ANFIS model (Ansari et al. 2010). In this study, the drought phenomenon in a series of time (276 months) was considered in one model of ANFIS neural networks in each station. The fuzzy system is a system based on the "conditional result" logical rule that, using the concept of linguistic variables and fuzzy decision-making process, depicts the space of input variables on the space of the output variables. A Sogno fuzzy system (this inference system is mostly used in control systems and in areas where mathematical calculations are required) with four inputs, one output, and two laws and an equivalent ANFIS system were presented. This system has two inputs x and y and one output (Ahmadzadeh et al. 2010). In the end, the error rate of the resulting models is compared and the function that obtains the lowest error rate at the lowest analyzing time was selected as a membership function (Konarkuhi et al. 2010). The model structure of the ANFIS (adaptive neuro-fuzzy inference systems) is shown in Fig. 3. The branches of this graph are encoded with circles. These circles specify the type of rules (or and or). The last node on the left is the input and the last node on the right is the output. The five-layer ANFIS structure described above is visible in this structure. In the surface viewer, different modes of output index in the form of fuzzy membership functions are displayed as well as changes in the values of the input index classes and can give more details of the level of changes in the new index between 0 and 1.

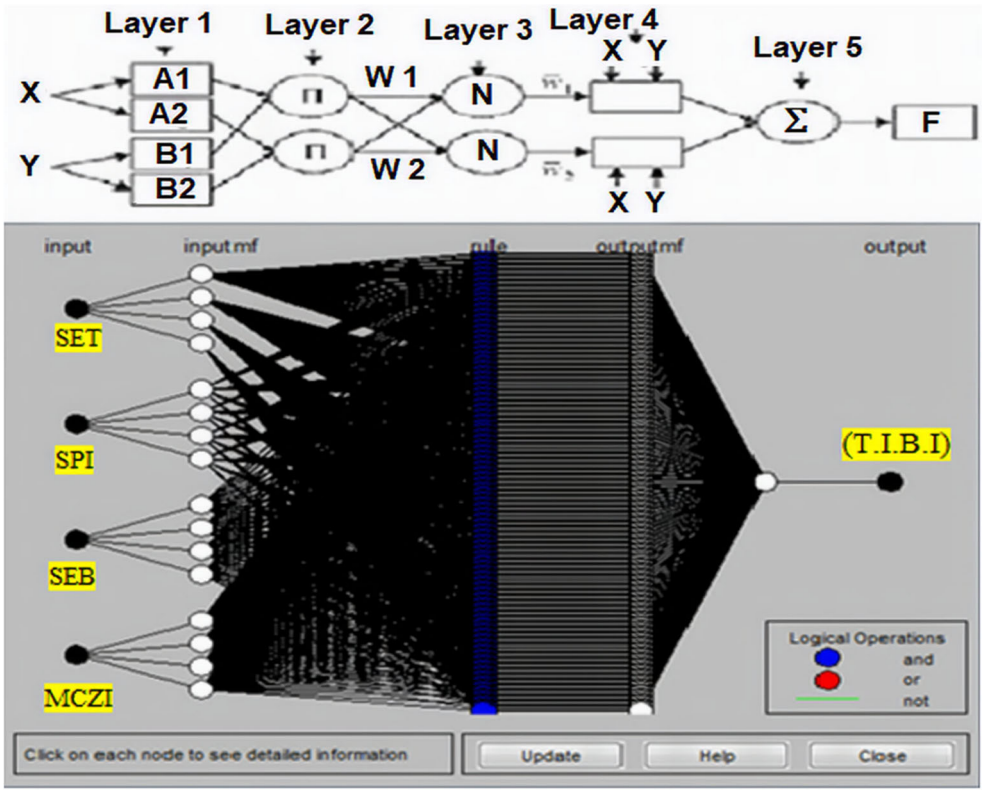

Fig. 3 ANFIS model structure

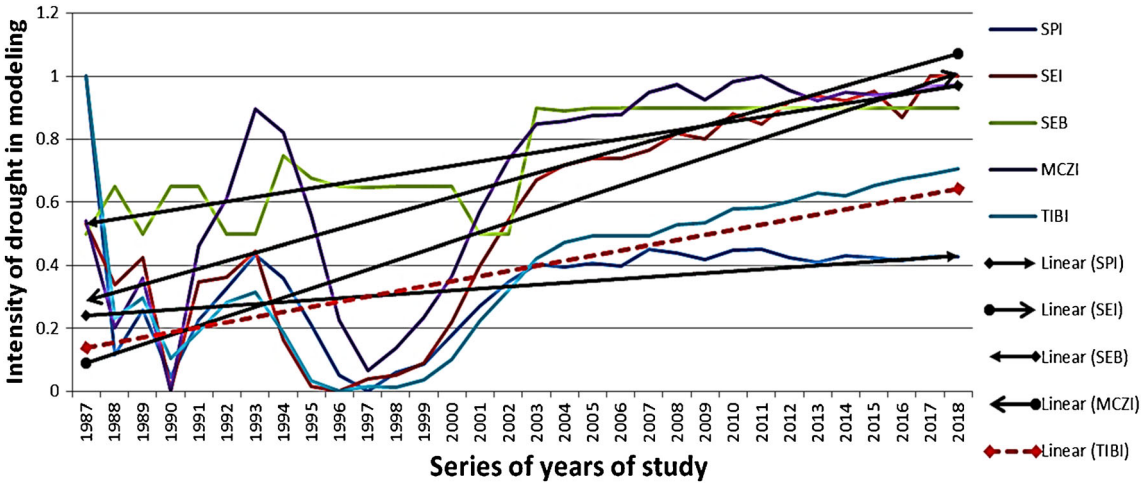

Fig. 4 The fluctuation of the indices at Tabriz station in the 6-month scale and statistical period of 2000–2018

Satellite datasets

MODIS is an extensive program that provides images in 36 spectral bands between 0.405 and 14.385 lm using sensors on two satellites—Terra and Aqua (Srivastava et al. 2013). MODIS images can be downloaded from the website https://lpdaac.usgs.gov/lpdaac/ products/modis_products_table. Global MODIS vegetation indices are designed to provide continuous spatial and temporal information of vegetation conditions (Lunetta et al. 2006). Global MOD13Q1 data are available on every 16 days basis at 250-m spatial resolution. It is a gridded level 3 product in the sinusoidal projection. The other important datasets required for any drought monitoring program is precipitation. For more accurate three-dimensional precipitation retrievals, the first-ever space-borne active microwave sensor, the precipitation radar (PR), was deployed along with the TRMM microwave imager (TMI) in 1997 (Huffman et al. 2007; Iguchi et al. 2000). TRMM 3B43 algorithm combines 3-hourly integrated high-quality data, infrared (IR) estimates, (3B42) with the monthly accumulated climate assessment monitoring system (Huffman et al. 1997, 2007). It has a limited earth view covering only the 38° N to 38° S (Gao et al. 2006). In this study, TRMM 3B43 multi-satellite precipitation analysis (TMPA) products were used to obtain the monthly data during the period of 1998–2008 in American Standard Code for Information Interchange (ASC2) format (Yaduvanshi et al. 2015; Rizky Aulia et al. 2016). Google Earth Engine combines a multi-petabyte catalogue of satellite imagery and geospatial datasets with planetary-scale analysis capabilities and makes it available for scientists, researchers, and developers to detect changes, map trends, and quantify differences on the Earth's surface.

Results and discussion

Monitoring of drought fluctuations based on four integrated indices in T.I.B.I

In order to investigate the effect of drought fluctuations on the conditions of the stations, it is possible to analyze the changes in the indicators (SET, SPI, SEB, and MCZI) as

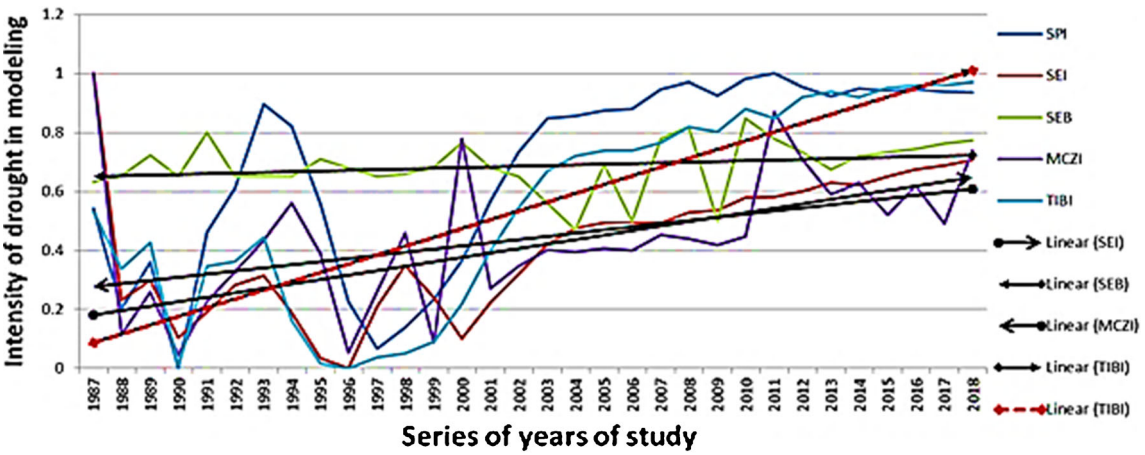

Fig. 5 The fluctuation of the indices at Tabriz station in the 12-month scale and statistical period of 2000–2018

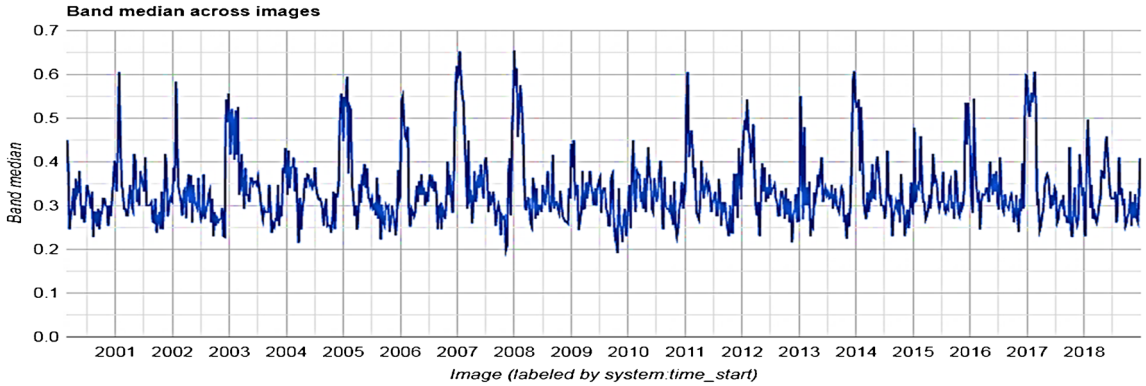

Fig. 6 Drought oscillation chart based on NDVI and Dev-NDVI index in the northern part of the study area (April 2000–2018)

appeared in the T.I.B.I. index. Considering a large number of stations, for the sake of better understanding, only the drought series graph of Tabriz station was presented in both 6- and 12-month scale (Figs. 4 and 5) (in these figures, the cross-sectional red line shows drought margin on a 6-month and more scale with the amount of 0.74 and a 12-month and more scale with the amount of 0.74). The analysis of these figures shows that at the 6- and 12-month scale at Tabriz station, the amount of evapotranspiration was similar in drought conditions, which decreased from March 1994 to July 1998, and after this month an increase was observed, while the impact of rainfall on a 6-month scale is weaker than the 12-month scale. It means that from April 1996 to December 2004, an increasing trend occurred and after that followed by the same pattern. The indicators (SET, SPI, SEB, and MCZI) affect the T.I.B.I. index and show somehow a trend, indicating that the new T.I.B.I fuzzy index reflects the four indicators well. The T.I.B.I index at the 12-month scale shows a sharper shape than the 6-month scale. According to the results of the new T.I.B.I fuzzy model, the intensity of drought is increasing in most of the studied stations. Also, based on the output of the mentioned model, the frequency of drought in the northwestern stations and the central part of the study area is high. Stations in the southern parts and the semi-eastern strip of the study area have lower drought intensity and frequency.

Analysis and monitoring of drought using MODIS and TRMM satellite data

In this section, due to the large study area, we divided it into three parts: the northern region (Ardabil, East and West Azerbaijan provinces); central (Zanjan, Kurdistan, Kermanshah, and Hamadan); and the southern (Khuzestan, Ilam, Lorestan). Then, for each part of drought monitoring, two indices—NDVI (normalized difference vegetation index) and Dev-NDVI (deviation from normalized difference vegetation index)—were evaluated. The product and images extracted from the MODIS and TRMM satellite for the years 2000 to 2018 were presented only for the month of April each year due to the high frequency. Monitoring in the northern part of the study area, based on NDVI and Dev-NDVI drought estimation indices, indicates increased drought stress. The intensity of the drought fluctuates from 2011 until 2018. This is visible in the drought oscillation chart in the northern part of the study area based on NDVI and Dev-NDVI index shown in Fig. 6. It is worth noting that the increase in drought estimation index of NDVI and Dev-NDVI is an increase in drought and a decrease in crop moisture and an increase in drought and conversely, the lower the drought estimation index of plants. The decreased moisture content of plants indicates a drought. The index used to monitor drought in the study area indicates this. Droughts have occurred in accordance with modelling.

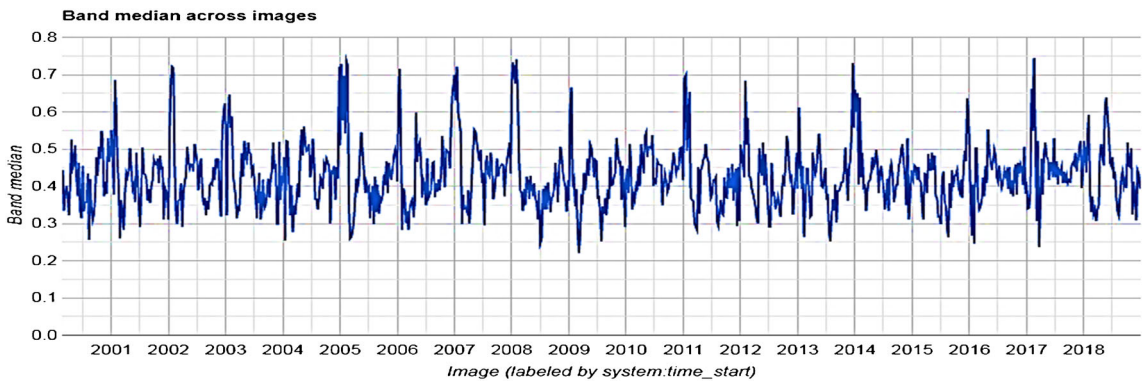

Fig. 7 Drought oscillation chart based on NDVI and Dev-NDVI index at the central part of the study area (April 2000–2018)

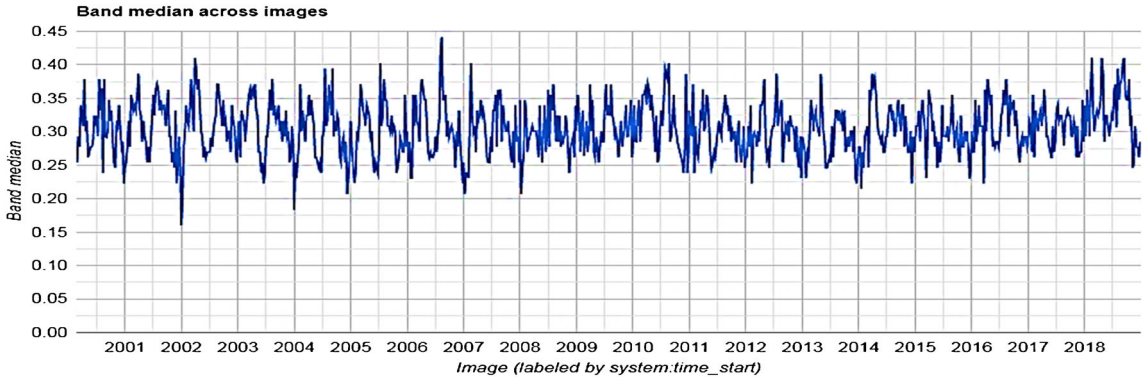

Fig. 8 Drought oscillation chart based on NDVI and Dev-NDVI index in the southern part of the study area (April 2000–2018)

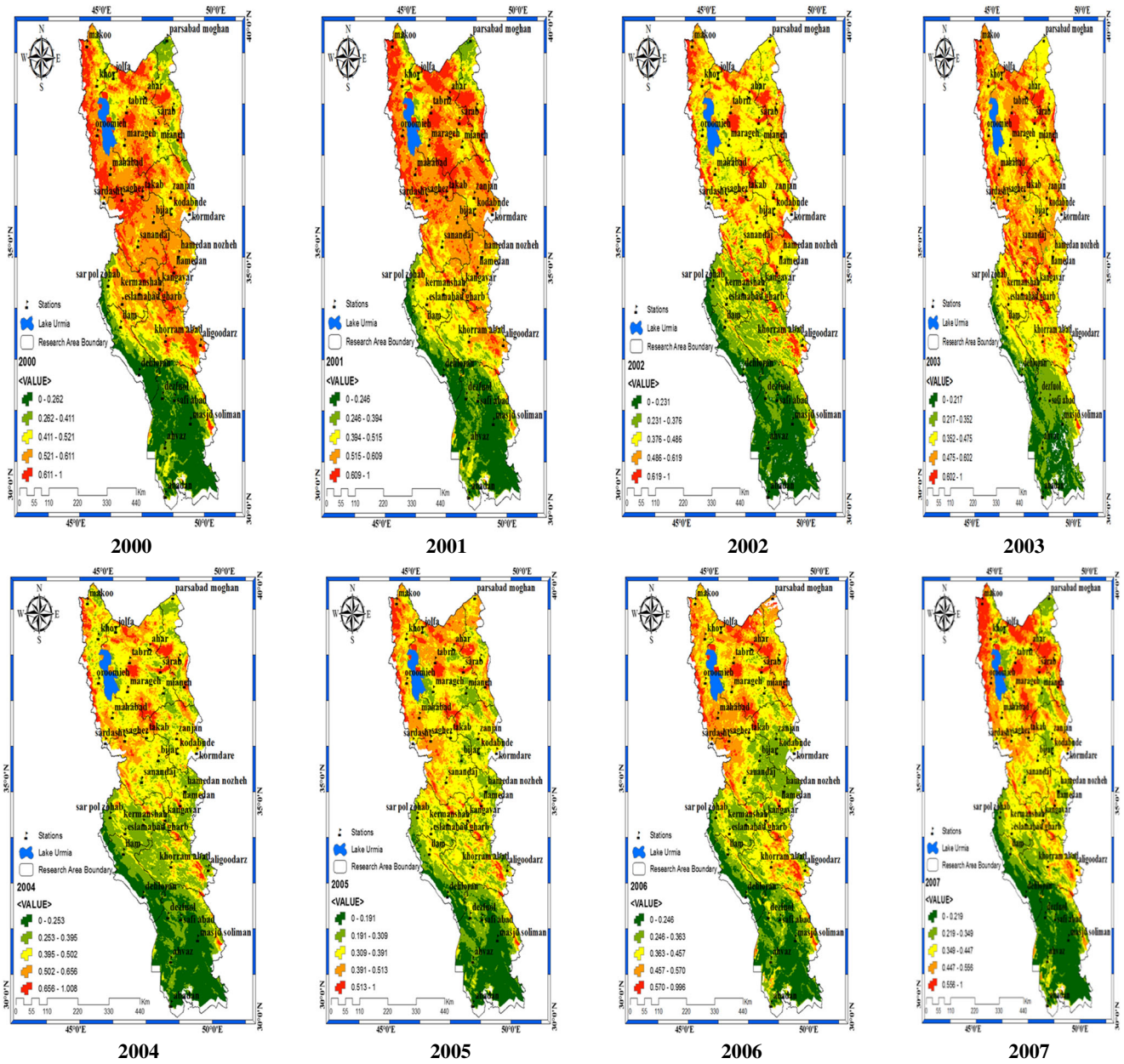

Fig. 9 The spatial pattern of drought in the study area based on NDVI and Dev-NDVI index extracted from MODIS and TRMM satellite data (April 2000–2018)

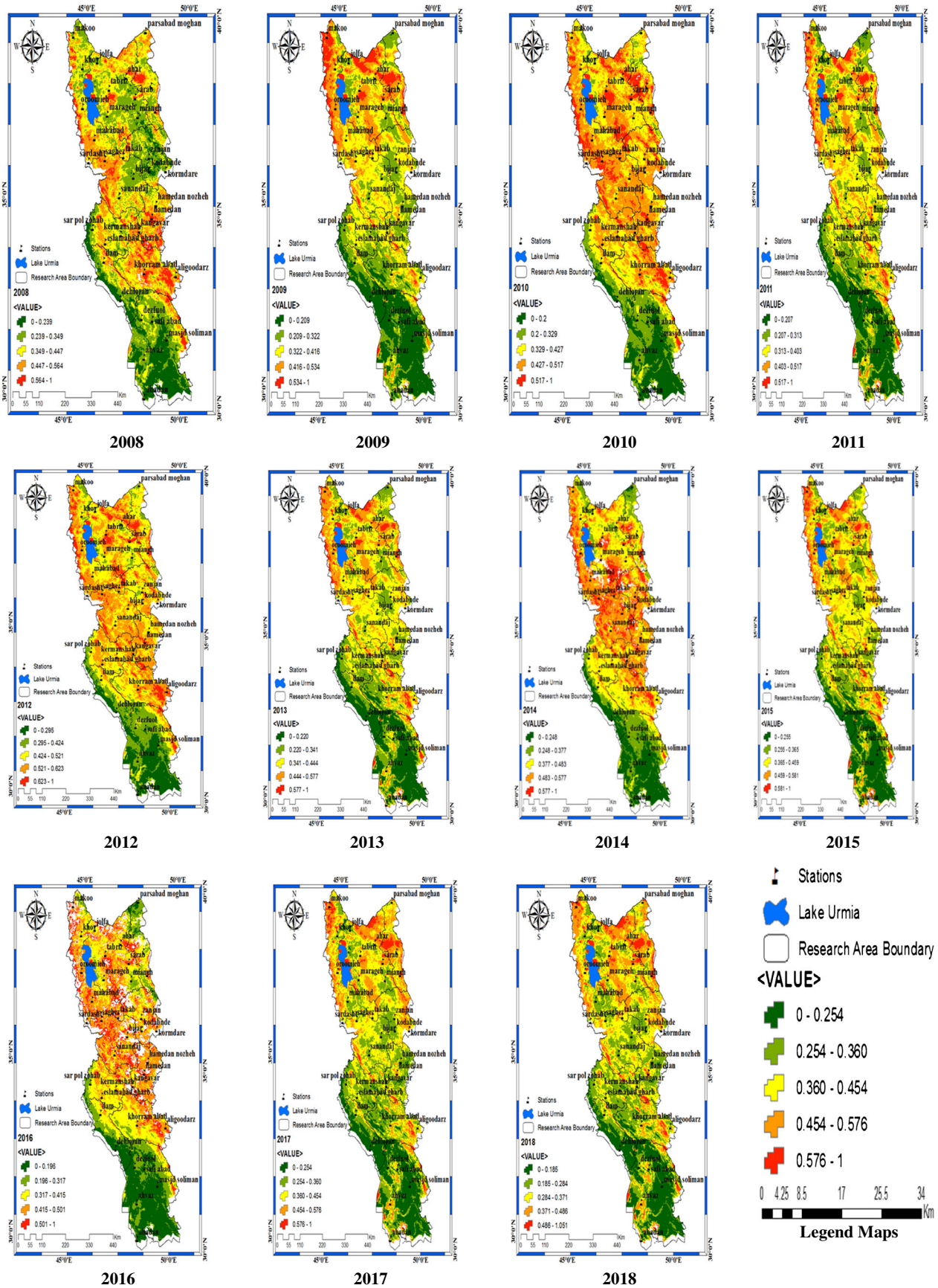

Fig. 9 (continued)

The obtained data can show the drastic fluctuation of droughts based on arable land estimation index. Especially in the recent years, from 2017 to 2018, its values have reached 0.79. This means that drought has occurred in the study area. This is visible in the drought oscillation chart in the central part of the study area based on NDVI and Dev-NDVI index shown in Fig.7. Drought spraying in the study area was based on NDVI and Dev-NDVI index. This drought index is more severe than the two study areas. That is, the drought range based on NDVI and Dev-NDVI index has been rising from 0.25 to 1 in most months of the year. And this increase indicates a decrease in the moisture content of crops and an increase in drought. This is visible in the drought oscillation chart in the southern part of the study area based on NDVI and Dev-NDVI index shown in Fig.8. According to the results of the TRMM satellite imagery data and MODIS sensor based on the two indicators (NDVI and Dev-NDVI), in the northern part of the study area during the study period 2000–2018, it had a high drought for 4 years (2000–2003). The southern basin of Lake Urmia had drought intensity levels close to 0.96–1%. While the drought has been partially reduced between 2004 and 2011, the drought has risen sharply again in 2010. During this period, i.e. 2004–2011, the northern and central part of the study area had a higher drought intensity than the other study area. Meanwhile, in the period from 2012 to 2018, the intensity of the drought has increased. In 2012, most areas except the southern part of the region were experiencing severe drought. While in 2016, the intensity of drought in the northern and eastern parts of the central part of the country has increased (refer to Fig. 9 for a visual overview of the satellite images of drought oscillation based on data from the Terra satellite and the MODIS sensor).

Conclusions

Drought has dramatic effects on the different parts of human life including economics, agriculture, environment, and so on. The results of the present study showed that the output of the high-level T.I.B.I fuzzy model corresponded with the MODIS and TRMM satellite image data output. The output of the T.I.B.I model reflects severe drought in the northern and central part of the study area. Satellite data outputs in April showed that since 2001 the intensity of the drought has begun and in 2010 its intensity has increased. The MODIS satellite output had a high accuracy compared with the TRMM satellite in the study area. Precipitation characteristics represent the highest amount of rainfall in the west, south, and east the study area is larger. Further, it was observed from the temporal variations of NDVI and Dev-NDVI that the agricultural drought had significantly influenced the northwestern as well as the central portion of the area of the study. The results of this study showed that TRMM and MODIS are reliable in output and monitoring in meteorological and agricultural drought assessment. This can be very effective in extracting endangered areas. According to the outputs of the TRMM and MODIS satellite products, the highest drought intensity is on the margins of Lake Urmia. The highest amount of precipitation and humidity in April was in 2006, 2008, 2009, and 2018. According to the findings of the T.I.B.I fuzzy model and the output of TRMM satellite images, the affected areas were characterized by high drought intensity which can be seen in Fig. 9. The results of the present study can be used in managing crises and natural hazards for officials and managers and reduce the damage caused by it.

In this research, we studied on monitoring and investigating the possibility of forecasting drought in the western part of Iran. This method has been used in many studies and it has been considered as a suitable method for monitoring, analysis, and comparison, for example, Alizadeh et al. (2017) in their research on the modeling of dispersion of droughts due to climate change in Iran by using a dynamical system; Zeinali and SafarianZengir (2017) in a study on drought monitoring in the Lake Urmia Basin using the fuzzy index that it had an acceptable; Fathizadeh et al. (2017) in a research on the relationship between meteorological drought and solar variables in some of Iran's interconnection stations and verified the efficiency of the models; Safarianzengir et al. (2019) in a study on modeling and monitoring of drought for forecasting it, to reduce natural hazards in the western and northwestern part of Iran; Sobhani et al. (2020a) in a study on investigating the effects of drought on the environment in the northwestern province of Ardabil, Iran, using combined indices; and finally Safarianzengir and Sobhani (2020) in a research on simulation and analysis of natural hazard phenomenon, drought in the southwest of the Caspian Sea. However, models in the present study were useful in monitoring and investigating the possibility of forecasting drought in the western part of Iran.

Acknowledgments The present article is extracted from the doctoral thesis of physical geography (climatology) in the University of Mohaghegh Ardabili, Ardabil, Iran, with title "Monitoring and forecasting drought in the western part of Iran". We also acknowledge the TERRA satellite and the MODIS sensor personnel and scientists for their efforts, data sharing, and for the production its.

Availability of data When the article will be accepted, the data used in this research will be released.

Compliance with ethical standards

Conflict of interests The authors declare that they have no conflict of interests.

Ethics approval and consent to participate This article is the product of the author's original results and all of them are familiar with the

publication of the *Arabian Journal of Geosciences*. This article has not been published yet in another magazine and is currently not being judged in any magazine.

Consent for publication All authors agree to publish the article after acceptance.

References

Ahmadzadeh G, Majid L, Kourosh M (2010) Comparison of artificial intelligence systems (ANN and ANFIS) in estimating the rate of transpiration of reference plants in very dry regions of Iran. J Water Soil 2(4):679–689 [In Persian]

Alizadeh S, Mohammadi H, Kordvani P (2017) Modeling the dispersion of drought caused by climate change in Iran using dynamic system. Land Expansion 9:169–188 [In Persian]

Ansari H, Davari K, Sanaeenejad SH (2010) Drought monitoring using SEPI standardized rainfall and sedimentation index, developed on the basis of fuzzy logic, Journal of Soil and Water (Agricultural Sciences and Technology), No. Pp 1:38–52

Bajgirana GE, Luca SDE (2008) Multilayer feedforward networks for transportation mode choice analysis: an analysis and a comparison with random utility models. Transportation research part C: Emerging Technologies 13:121–155

Borromeo E, Vadheim B, Woldeyes FB, Alamirew T, Tamura S, Charles KJ, Kebede S, Walker O (2018) The distributional and multi-sectoral impacts of rainfall shocks: evidence from computable general equilibrium modelling for the Awash Basin, Ethiopia. Ecological Economics, Elsevier, vol 146(C):621–632. https://doi.org/10.1016/j.ecolecon.2017.11.038

Campana PE, Zhang J, Yao T, Andersson S, Landelius T, Melton F, Yan J (2018) Managing agricultural drought in Sweden using a novel spatially-explicit model from the perspective of water-food-energy nexus. J Clean Prod 197:1382e1393

Cohn AS, Vanwey LK, Spera SA, Mustard JF (2016) Cropping frequency and area response to climate variability can exceed yield response. Nat Clim Chang 6:601–604

Corners H, Babel W, Willinghöfer S, Biermann T, Köhler L, Seeber E, Foken T, Ma Y, Yang Y, Miehe G (2016) Evapotranspiration and water balance of high-elevation grassland on the Tibetan Plateau. J Hydrol 533:557–566

Cunha A, Alvalá R, Nobre C, Carvalho M (2015) Monitoring vegetative drought dynamics in the Brazilian semiarid region. Agric For Meteorol 214–215:494–505

Dai A (2012) Increasing drought under global warming in observations and models. Nat Clim Chang 3(52):58. https://doi.org/10.1038/nclimate1633

Dai A (2013) Increasing drought under global warming in observations and models. Nat Clim Chang 3:52–58

Donohue RJ, Roderick ML, McVicar TR, Farquhar GD (2013) Impact of CO2 fertilization on maximum foliage cover across the globe's warm, arid environments. Geophys Res Lett 40:3031–3035. https://doi.org/10.1002/grl.50563

Fathizadeh H, Gholami-nia A, Mobin M, Soodyzizadeh H (2017) Investigating the relationship between meteorological drought and solar variables in some Iranian standards. Environ Hazards 17:63–87 [In Persian]

Feng Z, Chen Y, Zhang J, Guo E, Wang R, Li D (2019) Dynamic drought risk assessment for maize-based on crop simulation model and multi-source drought indices. J Clean Prod 233(2019):100e114. https://doi.org/10.1016/j.jclepro.2019.06.051

Fisher JB, Tu KP, Baldocchi DD (2008) Global estimates of the land-atmosphere water flux based on monthly AVHRR and ISLSCP-II data, validated at 16 FluxNet sites. Remote Sens Environ 112:901–919

Frankenberg C, Fisher JB, Worden J, Badgley G, Saatchi S, Lee J-E et al (2011) New global observations of the terrestrial carbon cycle from GOSAT: patterns of plant fluorescence with gross primary productivity. Geophys Res Lett 38:L17706. https://doi.org/10.1029/2011GL048738

Gao H, Wood E, Jackson T, Drusch M, Bindlish R (2006) Using TRMM/TMI to retrieve surface soil moisture over the southern United States from 1998 to 2002. J Hydrometeorol 7(1):23–38

Ghulam F, Najafi MS, Samadi M (2007) An analysis on synoptic patterns of springtime dust occurrence in west Iran. Physical Geography Research. 44:99–124. [In Persian]

Guan K, Berry JA, Zhang Y, Joiner J, Guanter L, Badgley G, Lobell DB (2016) Improving the monitoring of crop productivity using spaceborne solar-induced fluorescence. Glob Chang Biol 22:716–726

Guanter L, Alonso L, Gómez-Chova L, Amorós-López L, Vila-Francés J, Moreno J (2007) Estimation of solar-induced vegetation fluorescence from space measurements. Geophys Res Lett:34. https://doi.org/10.1029/2007GL029289

Guanter L, Frankenberg C, Dudhia A, Lewis PE, Gomez-Dans J, Kuze A et al (2012) Retrieval and global assessment of terrestrial chlorophyll fluorescence from GOSAT space measurements. Remote Sens Environ 121:236–251

Halwatura D, McIntyre N, Lechner AM, Arnold S (2017) The capability of meteorological drought indices for detecting soil moisture droughts. Journal of Hydrology, Regional Studies, pp 396–412

Han D, Wang G, Liu T, Xue B-L, Kuczera G, Xu X (2018) Hydroclimatic Response of Evapotranspiration Partitioning to Prolonged Droughts in Semiarid Grassland. J Hydrol. https://doi.org/10.1016/j.jhydrol.2018.06.048

Hao Z, AghaKouchak A (2013) Multivariate standardised drought index: a parametric multi-index model. Adv Water Resour 57:12–18

Harrison MT, Tardieu F, Dong Z, Messina CD, Hammer GL (2014) Characterizing drought stress and trait influence on maize yield under current and future conditions. Glob Chang Biol 20(3):867e878

Huffman GJ, Adler RF, Arkin P, Chang A, Ferraro R, Gruber A, Janowiak J, McNab A, Rudolf B, Schneider B (1997) The Global Precipitation Climatology Project (GPCP) combined precipitation dataset. B Am Meteorol Soc 78(1):5–20

Huffman GJ et al (2007) The TRMM multi-satellite precipitation analysis (TMPA): quasi-global, multiyear, combined-sensor precipitation estimates at fine scales. J Hydrometeorol 8(1):38–55

Iguchi T, Kozu T, Meneghini R, Awaka J, Okamoto Ki (2000) Rain-profiling algorithm for the TRMM precipitation radar. J Appl Meteorol 39(12):2038–2052

IPCC (2014) Climate Change 2014: impacts, adaptation, and vulnerability. Part B: regional aspects. Contribution of Working Group II to the Fifth Assessment Report of the Intergovernmental Panel on Climate Change. Cambridge University Press, Cambridge, United Kingdom and New York, NY, USA.

Jiao W, Zhang L, Chang Q, Fu D, Cen Y, Tong Q (2016) Evaluating an enhanced vegetation condition index (vci) based on viupd for drought monitoring in the continental United States. Remote Sens 8:224. https://doi.org/10.3390/rs8030224

Jiao W, Tian C, Chang Q, Novick KA, Wang L (2019a) A new multi-sensor integrated index for drought monitoring. Agric For Meteorol 268:74–85

Jiao W, Wang L, Novick KA, Chang Q (2019b) A new station-enabled multi-sensor integrated index for drought monitoring. J Hydrol. https://doi.org/10.1016/j.jhydrol.2019.04.037

Joiner J, Yoshida Y, Vasilkov AP, Yoshida Y, Corp LA, Middleton EM (2011) First observations of global and seasonal terrestrial chlorophyll fluorescence from space. Biogeosciences 8:637–651. https://doi.org/10.5194/bg-8-637-2011

Joiner J, Yoshida Y, Vasilkov AP, Middleton EM, Campbell PKE, Yoshida Y et al (2012) Filling-in of near-infrared solar lines by terrestrial fluorescence and other geophysical effects: simulations and space-based observations from SCIAMACHY and GOSAT. Atmospheric Measurement Techniques 5:809–829. https://doi.org/10.5194/amt-5-809-2012

Keyantash JA, Dracup JA (2004) An aggregate drought index: assessing drought severity based on fluctuations in the hydrologic cycle and surface water storage. Water Resour Res 40(9)

Kogan FN (1990) Remote sensing of weather impacts on vegetation in non-homogeneous areas. Int J Remote Sens 11:1405–1419. https://doi.org/10.1080/01431169008955102

Kogan FN (1997) Global drought watch from space. Bull Am Meteorol Soc 78(4):621–636

Kogan FN (2001) Operational space technology for global vegetation assessment. Bull Am Meteorol Soc 82:1949–1964

Konarkuhi A, SoleimanJahi H, Falahi S, Riahimadvar H, Meshkat Z (2010) Using the new intelligent fuzzy-neural recognition inventory system (ANFIS) to predict the human cannibalization potential of human papilloma virus. J Arak Univ Sci Technol 13(4):95–105 [In Persian]

Lee J-E, Frankenberg C, van der Tol C, Berry JA, Guanter L, Boyce CK, Fisher JB, Morrow E, Worden JR, Asefi S (2013) Forest productivity and water stress in Amazonia: observations from GOSAT chlorophyll fluorescence. Proc R Soc B Biol Sci 280:20130171

Li Y, Huang H, Ju H, Lin E, Xiong W, Han X, Wang H, Peng Z, Wang Y, Xu J, Cao Y, Hu W (2015) Assessing vulnerability and adaptive capacity to potential drought for winter-wheat under the RCP 8.5 scenario in the Huang-Huai-Hai Plain. Agric Ecosyst Environ 209: 125e131

Liu Y, Zhu Y, Ren L, Yong B, Singh VP, Yuan F, Jiang S, Yang X (2019) On the mechanisms of two composite methods for construction of multivariate drought indices. Sci Total Environ 647:981e991

Lu X, Wang L, McCabe MF (2016a) Elevated CO2 as a driver of global dryland greening. Sci Rep 6 (20716 EP)

Lu X, Wang L, Pan M, Kaseke KF, Li B (2016b) A multi-scale analysis of Namibian rainfall over the recent decade– comparing TMPA satellite estimates and ground observations. J Hydrol: Regional Stud 8:59–68

Lunetta RS, Knight JF, Ediriwickrema J, Lyon JG, Worthy LD (2006) Land-cover change detection using multi-temporal MODIS NDVI data. Remote Sens Environ 105(2):142–154

McVicar TR, Jupp DL (1998) The current and potential operational uses of remote sensing to aid decisions on drought exceptional circumstances in Australia: a review. Agric Syst 57:399–468. https://doi.org/10.1016/S0308-521X(98)00026-2

Mu Q, Zhao M, Kimball JS, McDowell NG, Running SW (2013) A remotely sensed global terrestrial drought severity index. Bull Am Meteorol Soc 94:83–98. https://doi.org/10.1175/BAMS-D-11-00213.1

Okotto L, Okotto-Okotto J, Price H, Pedley S, Wright J (2015) Socio-economic aspects of domestic groundwater consumption, vending and use in Kisumu, Kenya, Applied Geography, Volume 58. March 2015:189–197. https://doi.org/10.1016/j.apgeog.2015.02.009

Peters AJ, Walter-Shea EA, Lei J, Vina A, Hayes M, Svoboda MR (2002a) Drought monitoring with NDVI-based standardized vegetation index. Photogramm Eng Remote Sens 68:71–75

Peters AJ, Walter-Shea JL, Viña A, Svoboda MD (2002b) Drought monitoring with NDVI-based standardized vegetation index. Photogramm Eng Remote Sens 68:71–75

Piao S, Ciais P, Huang Y, Shen Z, Peng S, Li J, Zhou L, Liu H, Ma Y, Ding Y, Friedlingstein P, Liu C, Tan K, Yu Y, Zhang T, Fang J (2010) The impacts of climate change on water resources and agriculture in China. Nature 467(7311):43

Qian X, Qiu B, Zhang Y (2019) Widespread decline in vegetation photosynthesis in Southeast Asia due to the prolonged drought during the 2015/2016 El Niño. Remote Sens 11:910

Ray DK, Gerber JS, MacDonald GK, West PC (2015) Climate variation explains a third of global crop yield variability. Nat Commun 6(5989 EP)

Rizky Aulia M, Yudi Setiawan L, Fatikhunnada A (2016) Drought detection of West Java's paddy field using MODIS EVI satellite images (case study: Rancaekek and Rancaekek Wetan). Procedia Environ Sci 33:646–653 http://creativecommons.org/licenses/by-nc-nd/4.0/.

Rojas O, Vrieling A, Rembold F (2011) Assessing drought probability for agricultural areas in Africa with coarse resolution remote sensing imagery. Remote Sens Environ 115:343–352. https://doi.org/10.1016/j.rse.2010.09.006

Rouse JW Jr, Haas RH, Schell JA, Deering DW (1974) Monitoring vegetation systems in the great plains with ERTS. NASA Spec Publ 351:309

Safarianzengir V, Sobhani B, Asghari S (2019) Modeling and monitoring of drought for forecasting it, to reduce natural hazards atmosphere in western and north western part of Iran, Iran. Air Qual Atmos Health (2019). https://doi.org/10.1007/s11869-019-00776-8

Safarianzengir V, Sobhani B (2020) Simulation and analysis of natural hazard phenomenon, drought in Southwest of the Caspian Sea, IRAN. Carpathian J Earth Environ Sci 15(1):127–136. https://doi.org/10.26471/cjees/2020/015/115

Safarianzengir V, Sobhani B, Asghari S (2019) Modeling and monitoring of drought for forecasting it, to reduce natural hazards Atmosphere in western and north western part of Iran, Iran. Air Qual Atmos Health 2019. https://doi.org/10.1007/s11869-019-00776-8

Sandholt I, Rasmussen K, Andersen J (2002) A simple interpretation of the surface temperature/vegetation index space for assessment of surface moisture status. Remote Sens Environ 79:213–224. https://doi.org/10.1016/S0034-4257(01)00274-7

Sheffield J, Goteti G, Wen F, Wood EF (2004) A simulated soil moisture based drought analysis for the United States. J Geophys Res Atmos 109. https://doi.org/10.1029/2004JD005182 (n/a–n/a)

Sobhani B, Safarianzengir V (2019a) Modeling, monitoring and forecasting of drought in south and southwestern Iran, Iran. Model Earth Syst Environ 5. https://doi.org/10.1007/s40808-019-00655-2

Sobhani B, Safarianzengir V (2019b) Investigation hazard effect of monthly ferrrin temperature on agricultural products in north bar of Iran. Iraqi J Agric Sci 50(1):320–330

Sobhani B, Safarianzengir V (2020) Evaluation and zoning of environmental climatic parameters for tourism feasibility in northwestern Iran, located on the western border of Turkey. Model Earth Syst Environ (2020). https://doi.org/10.1007/s40808-020-00712-1

Sobhani B, Safarianzengir V, Kianian MK (2018) Potentiometric mapping for wind turbine power plant installation guilan province in Iran. J Appl Sci Environ Manag 22:1363–1368. https://doi.org/10.4314/jasem.v22i8.36

Sobhani B, Safarianzengir V, Kianian MK (2019a) Drought monitoring in the Lake Urmia basin in Iran. Arab J Geosci 12:448. https://doi.org/10.1007/s12517-019-4571-1

Sobhani B, Safarianzengir V, Kianian MK (2019b) Modeling, Monitoring and Prediction of Drought in Iran. Iranian (Iranica) J Energy Environ 10:216–224. https://doi.org/10.5829/ijee.2019.10.03.09

Sobhani B, Safarianzengir V, Miridizaj F (2019c) Feasibility study of potato cultivating of Ardabil province in Iran based on VIKOR model. Revue Agric 10(2):92–102

Sobhani B, Jafarzadehaliabad L, Safarianzengir V (2020a) Investigating the effects of drought on the environment in northwestern province of Iran, Ardabil, using combined indices. Iran Model Earth Syst Environ 2020. https://doi.org/10.1007/s40808-020-00733-w

Sobhani B, Safarianzengir V, Yazdani MH (2020b) Modelling, evaluation and simulation of drought in Iran, southwest Asia. J Earth Syst Sci 129:100 (2020). https://doi.org/10.1007/s12040-020-1355-7

Srivastava PK, Han D, Ramirez MA, Islam T (2013) Machine learning techniques for downscaling SMOS satellite soil moisture using MODIS land surface temperature for hydrological application. Water Resour Manag 27(8):3127–3144

Stosic T, Telesca L, Locia S, da Costa L, Stosic B (2015) Identifying drought-induced correlations in the satellite time series of hot pixels recorded in the Brazilian Amazon by means of the detrended fluctuation analysis. Physica A 233(2015):100e114. https://doi.org/10.1016/j.physa.2015.10.057

Sun Y, Fu R, Dickinson R, Joiner J, Frankenberg C, Gu L, Xia Y, Fernando N (2015) Drought onset mechanisms revealed by satellite solar-induced chlorophyll fluorescence: insights from two contrasting extreme events. J Geophys Res Biogeosci 120:2427–2440

Swapnil SV, Bhattacharya BK, Nigam R, Guhathakurta P, Kripan G, Chattopadhyay N, Gairola RM (2015) A combined deficit index for regional agricultural drought assessment over the semi-arid tract of India using geostationary meteorological satellite data. Int J Appl Earth Obs Geoinf 39(2015):28–39. https://doi.org/10.1016/j.jag.2015.02.009

Tadesse T, Brown JF, Hayes MJ (2005) A new approach for predicting drought-related vegetation stress: integrating satellite, climate, and biophysical data over the U.S. central plains. ISPRS J Photogrammetry Remote Sens 59(2005):244–253. https://doi.org/10.1016/j.isprsjprs.2005.02.003

Thenkabail O, Soleimanjahi H, Fallahi SH, RiahiMadvar H, Meshkat Z (2004) The application of the new intelligent Adaptive Nero Fuzzy Inference System (ANFIS) in prediction of human papilloma virus oncogenic potency. Journal of Arak University of Medical Science 4:95–105. [In Persian]

Thomas EA, Needoba J, Kaberia D et al (2019) Quantifying increased groundwater demand from prolonged drought in the East African Rift Valley. Sci Total Environ. https://doi.org/10.1016/j.scitotenv.2019.02.206

Trenberth KE, Dai A, Van Der Schrier G, Jones PD, Barichivich J, Briffa KR, Sheffield J (2014) Global warming and changes in drought. Nat Clim Chang 4:17

Tsakiris G, Pangalou D, Vangelis H (2007) Regional drought assessment based on the reconnaissance drought index (RDI). Water Resour Manag 21:821–833

Tucker (1979) Analysis and identification of synoptic patterns of dust storms in West of Iran. Journal of Geography and Environmental Hazards 5:119–105. [In Persian]

Wang P, Wen X, Gong J, Song C (2004) Vegetation temperature condition index and its application for drought monitoring. Proc IGRASS 2001(1):141–143

Wang L, D'Odorico P, Evans J, Eldridge D, McCabe M, Caylor K, King E (2012) Dryland ecohydrology and climate change: critical issues and technical advances. Hydrol Earth Syst Sci 16:2585–2603

Wang X, Guo W, Qiu B, Liu Y, Sun J, Ding A (2017a) Quantifying the contribution of land use change to surface temperature in the lower reaches of the Yangtze River. Atmos Chem Phys 17:4989–4996

Wang P, Tang J, Sun X, Wang S, Wu J, Dong X, Fang J (2017b) Heat waves in China: definitions, leading patterns, and connections to large-scale atmospheric circulation and SSTs. J Geophys Res Atmos 122:10–679

Wang X, Qiu B, Li W, Zhang Q (2019) Impacts of drought and heatwave on the terrestrial ecosystem in China as revealed by satellite solar-induced chlorophyll fluorescence. Sci Total Environ 693(2019):133627. https://doi.org/10.1016/j.scitotenv.2019.133627

Wilhelmi OV, Wilhite DA (2002) Assessing vulnerability to agricultural drought: a Nebraska case study. Nat Hazards 25(1):37–58

Worqlul AW, Jeong J, Dile YT, Osorio J, Schmitter P, Gerik T, Srinivasan R, Clark N (2017) Assessing potential land suitable for surface irrigation using groundwater in Ethiopia, Applied Geography, Volume 85. August 2017:1–13. https://doi.org/10.1016/j.apgeog.2017.05.010

Wu, J. et al., 2013. Establishing and assessing the integrated surface drought index (ISDI) for agricultural drought monitoring in mid-eastern China. Int J Appl Earth Obs Geoinf, 23(0): 397-410.

Yaduvanshi A, Srivastava PK, Pandey AC (2015) Integrating TRMM and MODIS satellite with socio-economic vulnerability for monitoring drought risk over a tropical region of India. Physics and Chemistry of the Earth xxx 2015:40–69. https://doi.org/10.1016/j.pce.2015.01.006

Yang J, Tian H, Pan S, Chen G, Zhang B, Dangal S (2018) Amazon drought and forest response: largely reduced forest photosynthesis but slightly increased canopy greenness during the extreme drought of 2015/2016. Glob Chang Biol 24:1919–1934

Yao N, Li Y, Lei T, Peng L (2018) Drought evolution, severity and trends in mainland China over 1961e2013. Sci Total Environ 616e617:73e89

Yoshida Y, Joiner J, Tucker C, Berry J, Lee J-E, Walker G, Reichle R, Koster R, Lyapustin A, Wang Y (2015a) The 2010 Russian drought impact on satellite measurements of solar-induced chlorophyll fluorescence: Insights from modeling and comparisons with parameters derived from satellite reflectances. Remote Sens Environ 166(2015):163–177. https://doi.org/10.1016/j.rse.2015.06.008

Yoshida Y, Joiner J, Tucker C, Berry J, Lee J-E, Walker G, Reichle R, Koster R, Lyapustin A, Wang Y (2015b) The 2010 Russian drought impact on satellite measurements of solar-induced chlorophyll fluorescence: insights from modeling and comparisons with parameters derived from satellite reflectances. Remote Sens Environ 166:163–177

Yuan X, Wei Y, Wang B, Mi Z (2017) Risk management of extreme events under climate change. J Clean Prod 166:1169e1174

Zambrano F, Lillo-Saavedra M, Verbist K, Lagos O (2016) Sixteen years of agricultural drought assessment of the BioBío Region in Chile using a 250 m resolution vegetation condition index (VCI). Remote Sens 8:530

Zambrano F, Vrieling A, Nelson A, Meroni M, Tadesse T (2018) Prediction of drought-induced reduction of agricultural productivity in Chile from MODIS, rainfall estimates, and climate oscillation indices. Remote Sens Environ 219(2018):15–30. https://doi.org/10.1016/j.rse.2018.10.006

Zeinali B, SafarianZengir V (2017) Drought monitoring in Urmia Lake Basin using fuzzy index. J Environ Risks 6:37–62. [In Persian]. https://doi.org/10.22111/jneh.2017.3075

Zhang A, Jia G (2013) Monitoring meteorological drought in semiarid regions using multi-sensor microwave remote sensing data. Remote Sens Environ 134:12–23. https://doi.org/10.1016/j.rse.2013.02.023

Zhang Q, Zhang J (2016) Drought hazard assessment in typical corn cultivated areas of China at present and potential climate change. Nat. Hazards 81(2):1323–1331

Zhang Q, Liu G, Hongbo Y, Bao Y (2016) Temporal and spatial dynamic of ET based on MOD16A2 in recent four years in Xilin Gol steppe. Acta Agrestia Sinica 24:286–293

Zhang L, Jiao W, Zhang H, Huang C, Tong Q (2017) Studying drought phenomena in the Continental United States in 2011 and 2012 using various drought indices. Remote Sens Environ 190:96–106

Zhao C, Liu B, Piao S, Wang X, Lobell DB, Huang Y, Huang M, Yao Y, Bassu S, Ciais P, Durand J-L, Elliott J, Ewert F, Janssens IA, Li T, Lin E, Liu Q, Martre P, Müller C, Peng S, Peñuelas J, Ruane AC, Wallach D, Wang T, Wu D, Liu Z, Zhu Y, Zhu Z, Asseng S (2017) Temperature increase reduces global yields of major crops in four independent estimates. Proc Natl Acad Sci 114:9326–9331. https://doi.org/10.1073/pnas.1701762114

Zhou L et al (2012) Comparison of remotely sensed and meteorological data-derived drought indices in mid-eastern China. Int J Remote Sens 33(6):1755–1779